Psychiatry Research 277 (2019) 45–51

Contents lists available at ScienceDirect

Psychiatry Research

journal homepage: www.elsevier.com/locate/psychres

Diffusion abnormalities in the corpus callosum in first episode schizophrenia: Associated with enlarged lateral ventricles and symptomatology☆

Elisabetta C. del Re[a,b], Sylvain Bouix[b], Jennifer Fitzsimmons[b], Gabriëlla A.M. Blokland[c], Raquelle Mesholam-Gately[d], Joanne Wojcik[d], Zora Kikinis[b], Marek Kubicki[b,e], Tracey Petryshen[c], Ofer Pasternak[b,f], Martha E. Shenton[b,e,f,g,1,*], Margaret Niznikiewicz[a,1]

[a] Laboratory of Neuroscience, Department of Psychiatry, VA Boston Healthcare System, Brockton Division, and Harvard Medical School, Boston, MA, USA
[b] Psychiatry Neuroimaging Laboratory, Department of Psychiatry, Brigham and Women's Hospital, and Harvard Medical School, Boston, MA, USA
[c] Psychiatric and Neurodevelopmental Genetics Unit, Department of Psychiatry and Center for Genomic Medicine, Massachusetts General Hospital, Harvard Medical School, Boston, MA, USA
[d] Commonwealth Research Center, Harvard Medical School, Boston, MA, USA
[e] Department of Psychiatry, Massachusetts General Hospital, Harvard Medical School, Boston, MA, USA
[f] Department of Radiology, Brigham and Women's Hospital, Harvard Medical School, Boston, MA, USA
[g] VA Boston Healthcare System, Brockton, MA, USA

ARTICLE INFO

Keywords:
First episode schizophrenia
Corpus callosum
Fractional anisotropy
Lateral ventricles

ABSTRACT

Introduction: Abnormalities in the corpus callosum (CC) and the lateral ventricles (LV) are hallmark features of schizophrenia. These abnormalities have been reported in chronic and in first episode schizophrenia (FESZ). Here we explore further associations between CC and LV in FESZ using diffusion tensor imaging (DTI).
Methods: . Sixteen FESZ patients and 16 healthy controls (HC), matched on age, gender, and handedness participated in the study. Diffusion and structural imaging scans were acquired on a 3T GE Signa magnet. Volumetric measures for LV and DTI measures for five CC subdivisions were completed in both groups. In addition, two-tensor tractography, the latter corrected for free-water (FA_t), was completed for CC. Correlations between LV and DTI measures of the CC were examined in both groups, while correlations between DTI and clinical measures were examined in only FESZ.
Results: Results from two-tensor tractography demonstrated decreased FA_t and increased trace and radial diffusivity (RD_t) in the five CC subdivisions in FESZ compared to HC. Central CC diffusion measures in FESZ were significantly correlated with volume of the LV, i.e., decreased FA_t values were associated with larger LV volume, while increased RD_t and trace values were associated with larger LV volume. In controls, correlations were also significant, but they were in the opposite direction from FESZ. In addition, decreased FA_t in FESZ was associated with more positive symptoms.
Discussion: Partial volume corrected FA_t, RD_t, and trace abnormalities in the CC in FESZ suggest possible de- or dys-myelination, or changes in axonal diameters, all compatible with neurodevelopmental theories of

☆ **For Monte and Sherry Buchsbaum:**

My husband, George, met Monte Buchsbaum moments before I did back in 1989 at the *International Congress for Schizophrenia Research* meeting at the Hotel Del Coronado in San Diego. I had left to find a colleague I was meeting, and my husband was standing at my poster waiting for me to return so we could leave together as I had put my poster up early. When I came back from meeting my colleague there was a man looking at my husband saying, "what are you doing with my images?" My husband saw me coming and said, "ask her, she is the owner of the poster." Monte turned to me and asked the same question. What I missed initially was that this was a compliment as he did not think anyone could make images of the brain as well as he had done back in 1989. So we talked in front of my poster and I was totally taken with his interest in science, in imaging, and in life. This was my first encounter with Monte, and I am fortunate to say that over the years I have had the pleasure of many more encounters that also included his wife, Sherry. Monte, Sherry, my husband and I shared many dinners together, with Monte always ready with the camera to take a picture of an exquisite morsel at a Michelin starred restaurant. These excursions took place in Vienna, Nice, Kyoto, and other restaurants around the world. It was always a delight to share a meal and an idea with Monte and Sherry. I hope to share many more dinners with them across many more continents.

Martha E. Shenton.

* Corresponding author.
E-mail address: Shenton@bwh.harvard.edu (M.E. Shenton).
[1] Shared Last Authorship.

https://doi.org/10.1016/j.psychres.2019.02.038
Received 5 February 2019; Received in revised form 16 February 2019; Accepted 16 February 2019
Available online 18 February 2019
0165-1781/

schizophrenia. Correlational findings between the volume of LV and diffusion measures in FESZ reinforce the concept of a link between abnormalities in the LV and CC in early stages of schizophrenia and are also compatible with neurodevelopmental abnormalities in this population.

1. Introduction

The corpus callosum (CC) is the largest white matter tract in the brain and it connects the left and the right hemisphere. Numerous studies have described structural abnormalities of the CC in first episode (FESZ) and in chronic schizophrenia, as well as in subjects at high risk for developing schizophrenia (e.g., Francis et al., 2011; Zhuo et al., 2016). A reduction in the midsagittal area of the CC is a consistent finding in chronic schizophrenia (Woodruff et al., 1995; Arnone et al., 2008), and volume decrease in one or more of the CC subdivisions have also been reported (e.g., Rotarska-Jagiela et al., 2008; del Re et al., 2016a; Francis et al., 2011).

In addition to volume abnormalities in CC, diffusion tensor imaging (DTI) derived CC abnormalities have also been investigated in schizophrenia (e.g., Whitford et al., 2012; Kubicki and Shenton, 2015). DTI is a relatively new imaging technique that quantifies the direction of the movement of water molecules, which in the human brain is more restricted in white matter fibers compared to gray matter or cerebrospinal fluid (CSF; e.g., Basser et al., 1994). Restriction that varies depending on the direction is referred to as fractional anisotropy (FA), and is a commonly used diffusion measure (e.g., Fitzsimmons et al., 2013). Other diffusion measures, albeit less frequently reported in the literature, include: 1) axial diffusivity (AD), which quantifies the movement of water in the direction of the axon (parallel), 2) radial diffusivity (RD), which quantifies the movement of water that is perpendicular to the direction of the axon, and trace, which quantifies the average movement of water across the entire image voxel (see review in Kubicki et al., 2007; see also Song et al., 2002, 2003, 2005).

A further important advance afforded by DTI is that microstructural changes in the brain can be quantified. In schizophrenia, *macrostructural* alterations in the brain, including volume, area, and cortical thickness measures, are likely a later outcome of a more subtle process that affects *microstructure* first. Thus, a focus on more microstructural alterations is critical for understanding the underlying neurobiology. Since microstructural changes in both gray matter and white matter reflect more subtle abnormalities they could potentially point to specific pathologies. Therefore, identifying such microstructural abnormalities, as opposed to macrostructural changes that are likely identified later in the course of the illness, can lead to the development of promising and novel treatment interventions.

Moreover, with the advent of DTI, there has been a shift in focusing almost exclusively on gray matter abnormalities in schizophrenia to focusing also on white matter abnormalities. Existing studies, however, report conflicting findings in diffusion measures of the CC in both chronic and FESZ (e.g., Price et al., 2005, 2007; Kubicki et al., 2008; Balevich et al., 2015; Buchsbaum et al., 2006; Dekker et al., 2010; Lee et al., 2013; Federspiel et al., 2006; Delisi et al., 1997).

In the current study, we present findings resulting from diffusion tensor analyses of the CC in FESZ and in healthy control (HC) subjects using two-tensor tractography (Malcolm et al., 2010). Two-tensor tractography overcomes some of the uncertainty of white matter tract reconstruction based on one-tensor tractography, as it is based on the direction of not just one but a second tensor in each voxel to quantify the motion of water. Two-tensor tractography also includes *a priori* knowledge of the preceding portion of the tract in estimating the fiber path (Malcolm et al., 2010). By employing two tensors instead of one, this technique also makes it possible to estimate diffusion measures in crossing fibers, a measurement not possible using one-tensor tractography. Additionally, because CSF has been shown to affect diffusion measures in areas that are in close proximity to CSF, and are thus prone to CSF contamination, such as fibers close to the lateral ventricles (LV) (Metzler-Baddeley et al., 2012), in this study we combine two-tensor tractography with free-water elimination to correct for CSF contamination in the CC, which borders the LVs (Baumgartner et al., 2012). Modeling of free-water was developed by Pasternak et al., (2009), and has been applied to investigate free-water, and free-water elimination (water bound to tissue) in both FESZ and chronic schizophrenia (Pasternak et al., 2012, 2015).

With respect to LV and CC abnormalities, these anatomical regions are midbrain structures that are closely linked in their development, where there is an inverse correlation between enlarged LV volume and decreased volume of central CC in FESZ (e.g., del Re et al., 2016a). Further, CC and LV share a strong genetic link (Pfefferbaum et al., 2000; Narr et al., 2000). For example, neurodevelopmental syndromes such as agenesis, or partial agenesis of the CC, or Pitt-Hopkins syndrome, which are highly heritable, are characterized by abnormalities in both of these midbrain structures (Paul, 2011).

By employing advanced DTI methods to characterize white matter properties of the CC in the current study, our goal was to determine whether or not there is a correlation between LV volume abnormalities and CC diffusion measures, where the latter indexes the microstructure of white matter tracks constituting the CC. Based on findings reported in the literature, of a strong correlation between volumetric abnormalities in the CC and the LV, including our study in FESZ (del Re et al., 2016a), we investigated the association between LV and CC diffusion abnormalities in FESZ.

2. Materials and methods

2.1. Participants

Sixteen patients diagnosed with FESZ (3/16 females), and 16 healthy controls (HC; 7/16 females), were recruited as part of the Boston Center for Intervention Development and Applied Research (CIDAR) study (www.bostoncidar.org), "Vulnerability to Progression in Schizophrenia." As this is a general protocol used for describing the subjects and measures for CIDAR, we use many of the same descriptions here as have been reported elsewhere (e.g., del Re et al., 2016a). HC were recruited from the general community via Internet advertisements. FESZ were recruited from local hospitals and outpatient clinics affiliated with Harvard Medical School, or through referrals from clinicians. The study was approved by the local IRB committees at Harvard Medical School, Beth Israel Deaconess Medical Center, Massachusetts General Hospital, Brigham and Women's Hospital, and the Veteran Affairs Boston Healthcare System (Brockton campus). All study participants gave written informed consent and received payment for participation.

HC were drawn from the same geographic base as the FESZ group with comparable age, gender, race and ethnicity, handedness, and parental socioeconomic status (PSES). No HC met criteria for any current major DSM-IV-TR Axis I disorders, or history of psychosis, Major Depression (recurrent), Bipolar disorder, Obsessive Compulsive Disorder, Post Traumatic Stress Disorder, or developmental disorders. Controls were also excluded for a history of psychiatric hospitalizations, prodromal symptoms, schizotypal or other Cluster A personality disorders, first degree relatives with psychosis, or any current or past use of antipsychotics (other past psychotropic medication use was acceptable, but the subjects must have been off medicine for at least 6 months before participating in the study, except for as needed medications like sleeping medications or anxiolytic agents, such as beta-blockers for

performance anxiety, tremors, etc.). Exclusion criteria for all participants were: sensory-motor handicaps, neurological disorders, medical illnesses that significantly impair neurocognitive function, diagnosis of mental retardation, education less than 5th grade if under 18 or less than 9th grade if 18 or above, not fluent in English, DSM-IV-TR substance abuse in the past month, DSM-IV-TR substance dependence, excluding nicotine, in the past 3 months, current suicidality, no history of ECT within the past five years for patients and no history of ECT ever for controls, or study participation by another family member.

Clinical diagnoses were based on interviews with the Structured Clinical Interview for DSM-IV-TR (SCID), Research Version (First et al., 2002) or the Kid-SCID (Hien et al., 1994) for subjects <18, as well as information from available medical records. All FESZ participants met DSM-IV-TR criteria for either schizophrenia ($N = 13$), schizoaffective disorder ($N = 2$) or schizophreniform disorder ($N = 1$). Clinical symptoms for patients were rated using the Brief Psychotic Rating Scale (Overall et al., 1961). For the patient group, the average time between first hospitalization and entry into the study was 0.7 ± 0.7 years (range 0.0–2.0 years).

All participants were evaluated using the Global Assessment of Functioning (GAF) scale (Jones et al., 1995). Parental socioeconomic status (PSES) was assessed using the Hollingshead two-factor index (Hollingshead, 1975). Premorbid intellectual abilities were estimated using the Reading subtest of the Wide Range Achievement Test-4 (WRAT-4) (Wilkinson and Robertson, 2006) and current intellect was estimated using the Vocabulary and Block Design subtests of the Wechsler Abbreviated Scale of Intelligence (WASI) (Wechsler, 1999). Twelve of 16 FESZ were medicated at time of testing. Medication dosage was estimated using chlorpromazine (CPZ) equivalents (see Table 1) No significant correlations were found between CPZ equivalents and diffusion or volumetric measures (p values ranging from 0.06 to 0.99).

All demographic and clinical data are summarized in Table 1.

2.2. MRI image acquisition

2.2.1. Imaging parameters

MRI scanning was performed at the Brigham and Women's Hospital in Boston, MA with a 3 Tesla General Electric Signa System (GE Medical Systems). High spatial resolution MR sequences included 3D T1-weighted [inversion recovery spoiled gradient recalled (SPGR)], 3D T2-weighted (CUBE), and diffusion acquisitions. The IR-SPGR sequence had a repetition time (TR) of 7.8 ms, an echo time (TE) of 3 ms, an inversion time of 600 ms, a 10° flip angle, a field of view (FOV) of 256 × 256 mm, a matrix size of 256 × 256, 176 slices, and 1 mm slice thickness. The 3D T2-weighted sequence had a TR of 3 s, a TE of 90 ms, a 90° flip angle, a FOV of 256 × 256 mm, a matrix size of 256 × 256, 176 slices, and 1 mm slice thickness. The high-resolution diffusion acquisition was twice refocused and had a TR of 17 s, TE 78 ms, a 90° flip angle, a FOV of 240 × 240 mm, a matrix size of 144 × 144, 85 slices, 1.7 mm slice thickness, 51 gradient directions with a b-value of 900 s/mm2, and eight additional non-diffusion-weighted (b0) images. We used the proprietary GE DTI sequence, which on a 3 T GE scanner minimizes TE for each subject.

2.3. MRI image processing

For structural data, each MRI scan was visually inspected for movement artifacts. Images were realigned to the anterior commissure-posterior commissure (AC-PC) line and to the sagittal sulcus to correct for head tilt. Multi-atlas brain segmentation (del Re et al., 2016b) was employed to automatically mask the brain. FreeSurfer 5.3 (Fischl et al., 2002) was employed to segment the scans.

LV volume was derived as described in detail in del Re et al., (2016a). Briefly, relative volumes were calculated by dividing the volumes by the Intracranial Content (ICC) value for each subject (Fig. 1).

For diffusion processing, each raw image was processed for noise reduction, eddy current correction and head motion correction. In reconstructing regions of interest (ROIs), tensors were estimated by the least squares method (Basser and Jones, 2002) using 3DSlicer software version 4.3.1 (http://www.slicer.org/) (Pieper et al., 2004; 2006).

The CC was reconstructed using ROIs based on the estimated tensor image using 3Dslicer software (Fig. 2 **A and B**). Individual ROIs were drawn as defined by Hofer (Hofer and Frahm, 2006). The resulting CC topography divides the CC into 5 regions as shown in Fig. 1. These regions include the anterior (region 1), mid-anterior (region 2), central (region 3), mid-posterior (region 4), and posterior CC (region 5). The anterior and mid-anterior CC comprises the anterior half of the CC while the central, mid-posterior and posterior portions of the CC cover the remaining half of the CC. The five CC regions closely match the CC subdivisions obtained using FreeSurfer (see del Re et al., 2016a).

We manually drew an inclusion ROI on color-by-orientation label maps over the mid-sagittal CC based on the following anatomy. The CC crosses the hemispheres in the mid sagittal plane from left to right and appears as red voxels on color-by-orientation label maps (Fig. 2**A**). The inclusion ROI had a width of 3 voxels and in order to capture the CC of both cerebral hemispheres, the ROI was drawn on three slices to the left and three slices to the right of the mid-sagittal slice. Voxels defined by the inclusion ROIs were used as seeds to perform the Unscented Kalman Filter, UKF, tractography.

2.4. Fiber tracking

In the first step, all possible tracts in the brain were reconstructed individually in native DWI space using the UKF Tractography library (Malcolm et al., 2010), which is part of the Slicer 3D software package (http://www.slicer.org). The UKF algorithm simultaneously tracts fibers while estimating a diffusion model. Here we chose a three-compartment model of two diffusion tensors and one free-water compartment with the following parameter settings: 1 seed point per voxel, minimum free-water volume corrected FA = 0.15, step length 0.3 mm. The results of this algorithm are FA, trace, axial and radial diffusivity (AD, RD) values that resolve crossing fibers and are corrected for free-water (Baumgartner et al., 2012; FA_t, $trace_t$, AD_t, RD_t). The correction for free-water, defined as isotropic water not constrained by tissue, such as in the CSF or in interstitial plasma, allows for a more precise and specific measurement of diffusivity than conventional DTI measures (Pasternak et al., 2012; Pasternak et al., 2018).

Tracts were visualized and checked for consistency. The final output of the tractography analysis was the mean value of FA_t, $trace_t$, AD_t and RD_t over the identified tract, where the small t indicates the free-water corrected scalar measure.

Table 1
Socio-demographic and clinical Information.

	HC ($N = 16$)	FESZ ($N = 16$)	F	p
Mean age (SD)	21.9 (3.6)	22.6 (4.0)	0.295	0.59
Gender (male/female)	9/7	13/3	—	0.25
Pre-morbid IQ (WRAT reading)	109.0 (16.1)	114.0 (14.8)	0.74	0.40
Current IQ	119.9 (13.9)	111.1 (12.4)	3.6	0.07
Parental SES	1.94 (0.93)	2.0 (0.97)	0.04	0.85
Interval MRI-first hospitalization (years)	—	0.7 (0.7)	—	N.A.
CPZ baseline	—	307.9 (191.9)	—	N.A.
BPRS positive baseline	—	6.63 (3.4)	—	N.A.
BPRS negative baseline	—	5.5 (2.4)	—	N.A.
GAF baseline	82.5 (10.3)	50.7 (8.6)	90.2	<0.01

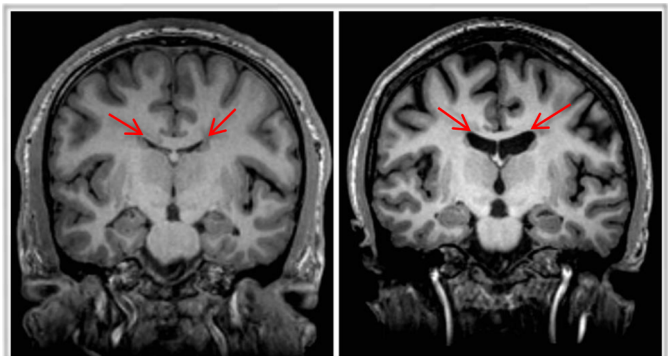

Fig. 1. A. Coronal T1-weighted MRI slice of a representative control subject and **B.** of a representative FESZ patient. Arrows indicate the CC and LV.

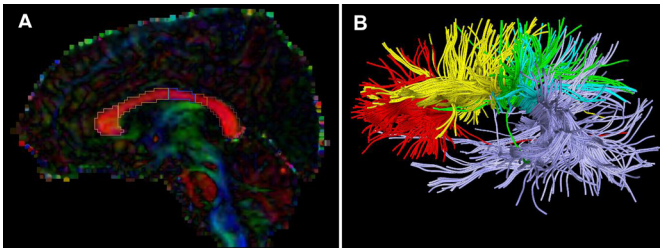

Fig. 2. Sagittal view of **A.** the DTI image of a control subject showing ROI seeding of the CC. **B.** Two-tensor tractography of the CC. The central CC is in bright green. (For interpretation of the references to color in this figure legend, the reader is referred to the web version of this article.)

2.5. Statistical analyses

All statistical analyses were performed with SPSS v.23, the exception being effect sizes, which were calculated with G*Power 3.1, 2009 (Faul et al., 2007). FA_t, $trace_t$, AD_t and RD_t, were analyzed in four different repeated measures MANOVAs that included Group and gender as a between-subjects factor and the five regions of the CC (anterior, mid-anterior, central, mid-posterior, posterior) as within-subjects factors.

2.6. Correlation analyses between CC diffusion measures and volume of the LV

The possible relationships between FA_t, RD_t, AD_t and $trace_t$ in the five CC subdivisions and volume of the bilateral LV were explored using correlation analyses and by calculating Pearson's *r*. We also computed Fisher's Exact Test for comparison of significant group differences in the pattern of correlations in patients and controls for the 4 diffusion measures for the central CC and LV volume. Only significant correlation results are reported below.

2.7. Correlation analyses between FA_t and clinical measures

Clinical correlations were limited to total positive and total negative symptom scores on the BPRS scale and FA_t of the five CC subdivisions. All correlations were computed using Pearson's *r*. A chi-square test was used to compare categorical data. Only significant correlations are reported below.

3. Results

3.1. Subject group characteristics

FESZ and control groups did not differ in age, years of education, premorbid IQ, current IQ or distribution of gender in the two groups (see Table 1). As expected, significant group differences were found in Global Assessment of Functioning, GAF, with lower mean GAF score in patients compared with HC.

3.2. Diffusion measures

Repeated measures MANOVA analysis demonstrated a main effect of Group for FA_t [$F(1,28) = 11.57$; $p = 0.002$], where FA_t was decreased in FESZ compared to HC. There was no main effect of gender [$F(1,28) = 0.65$; $p = 0.43$], nor a significant group by gender interaction [$F(1,28) = 0.09$; $p = 0.76$]. There was also no significant interaction of Group by CC sub-regions [$F(4,27) = 0.69$; $p = 0.68$].

RD_t and $trace_t$ were both significantly increased in FESZ compared to controls in the repeated measures MANOVA [$F(1,28) = 12.3$; $p = 0.002$] and [$F(1,28) = 9.79$; $p = 0.004$], respectively. There was no main effect of gender for RD_t [$F(1,28) = 0.81$; $p = 0.38$], nor a

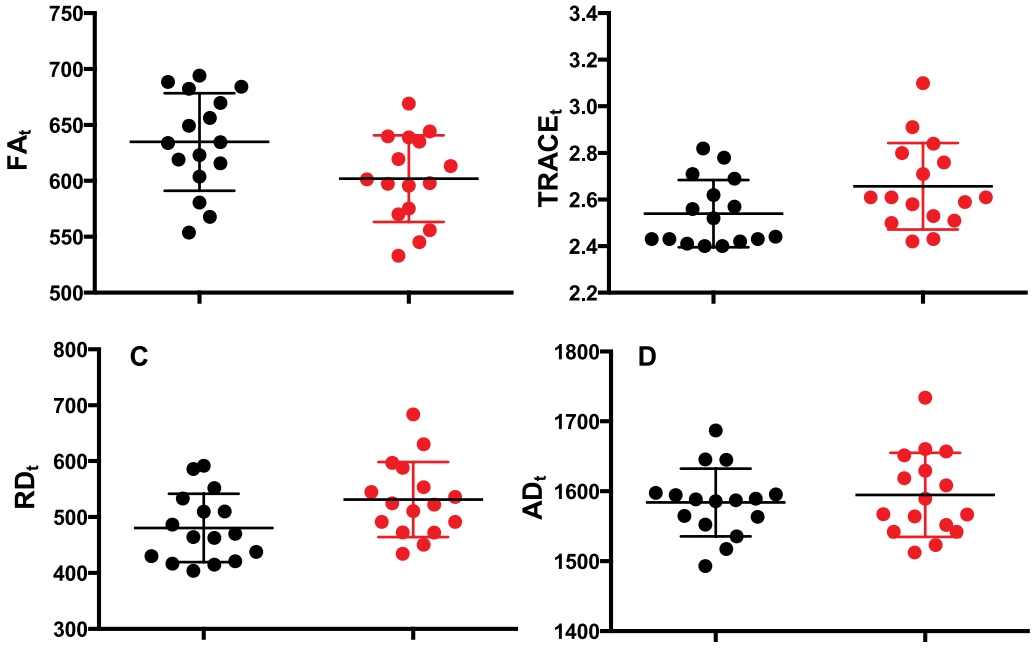

Fig. 3. A. FA_t, **B.** $trace_t$, **C.** RD_t, **D.** AD_t. All diffusion indices were measured with two-tensor tractography and were free-water corrected. HC (black) and FESZ (red). FA_t is significantly decreased ($p = 0.001$), while RD_t ($p = 0.001$) and $trace_t$ ($p = 0.001$) were significantly increased in FESZ compared to HC, with no group effects in AD_t ($p = 0.11$). (For interpretation of the references to color in this figure legend, the reader is referred to the web version of this article.)

significant group by gender interaction [F(1,28) = 0.08; $p = 0.78$]. Likewise, there was no main effect of gender for $trace_t$ [F(1,28) = 0.04; $p = 0.51$], nor a significant group by gender interaction [F(1,28) = 0.23; $p = 0.64$]. Neither RD_t nor $trace_t$ demonstrated a significant interaction of Group by CC sub-regions [F(4,27) = 0.7; $p = 0.58$; F(4,27) = 0.84; $p = 0.51$], respectively.

Additionally, there was no significant main effect of Group [F(1,28) = 1.23; $p = 0.28$], gender [F(1,28) = 0.11; $p = 0.75$], a significant group by gender interaction [F(1,28) = 1.19; $p = 0.28$], nor a significant interaction between Group and CC sub-regions for AD_t [F(4,27) = 0.77; $p = 0.55$] (see Figs. 2 and 3**).**

3.3. Correlations between CC diffusion measures and volume of the bilateral LV

In FESZ, volume of bilateral LV was significantly and inversely correlated with central CC FA_t ($r = -0.51$; $p < 0.05$) and significantly and positively correlated with central CC RD_t ($r = 0.5$, $p < 0.05$) and $trace_t$ ($r = 0.5$, $p < 0.05$); thus, larger LV volume correlated with decreased FA_t and increased RD_t and $trace_t$ values. In addition, a positive correlation with $trace_t$ ($r = 0.5$; $p < 0.047$) was observed in the mid-anterior CC region.

In controls, on the other hand, there was a positive correlation observed between the volume of the bilateral LV and FA_t measured in the central ($r = 0.7$; $p < 0.01$) and mid-posterior CC ($r = 0.55$, $p < 0.05$); and inverse correlations with RD_t of central ($r = -0.7$; $p < 0.01$) and posterior CC ($r = -0.6$, $p = <0.05$) as well as with $trace_t$ of central ($r = -0.65$, $p < 0.01$) and posterior CC ($r = -0.7$, $p < 0.01$). Thus, in controls, larger LV volume was associated with increased FA_t values, and decreased RD_t and $trace_t$ values (Fig. 3). Fisher's test for the group differences in the observed correlations showed significant effects for FA_t ($p = 0.0026$), RD_t ($p = 0.0003$) and $trace_t$ ($p = 0.006$).

Fig. 4.

3.4. Correlations between CC FA and clinical scales in FESZ

There were statistically significant negative correlations between BPRS total score for positive symptoms and FA_t of the central CC ($r = -0.55$; $p < 0.05$) (Fig. 5) and with FA_t of the adjacent mid-posterior region of the CC ($r = -0.5$, $p < 0.05$). These correlations suggest that decreased FA_t of the central and mid-posterior portions of the CC are associated with more positive symptom scores in FESZ.

4. Discussion

We used a combination of two-tensor tractography and a correction for free-water (Baumgartner et al., 2012) to obtain an accurate assessment of white matter abnormalities in the CC of FESZ (~0.7 months after first psychotic outbreak). Both of these methodological advances are important in the study of CC as the CC structure intersects with many other fiber bundles and is adjacent to the LVs. Findings demonstrate diffusion abnormalities in the five subdivisions of CC in FESZ. Of note, robust correlations between diffusion measures and LV were observed only for the central CC and not for other subdivisions within the CC. Moreover, FA_t abnormalities in FESZ were associated with more positive symptoms.

More specifically, we found that FA_t was significantly decreased, and RD_t, and $trace_t$ significantly increased in FESZ in all five CC subdivisions, while AD_t was unaffected. These abnormalities are indicative of the types of disease-related CC changes in FESZ. Of note, decreased FA has been associated with the degree of organization in white matter (Basser et al., 1994; Basser and Pierpaoli, 1996), while increased RD suggests de-myelination (Song et al., 2002, 2003, 2005). Thus, while decreased FA (including FA_t which is more tissue related) indicates more non-specific changes in white matter microstructure, increased RD in FESZ relative to HC, suggests possible de-myelination in the CC in FESZ.

The current findings of decreased FA_t and increased RD_t in FESZ also fit well with the existing literature on CC development. Of particular interest here, increased myelination has been hypothesized to be the main mechanism contributing to CC growth and to cognitive capacity development (Luders et al., 2007; Luders et al., 2011; Hutchinson et al., 2009). Of further note, it has been shown that the size of the CC in normal populations increases throughout late adolescence (Giedd et al., 1996), the mid-twenties (Pujol et al., 1993), and into middle-age (Prendergast et al., 2015), likely due to continued myelination. In contrast, Keller et al., (2003) reported that CC growth trajectory in childhood-onset schizophrenia shows a decline starting at 22 years of age compared to continuing growth in healthy controls. In our previous study (del Re et al., 2016a), we observed volume reduction in central CC in FESZ, which remained stable at one-year follow-up. A decrease of white matter in the anterior CC, but not other portions of the CC, in early schizophrenia over the first five-year period has also been shown by de Moura (2018). These findings, taken together with findings from the current study, suggest that the observed reduction in CC volume reported across several previous studies may be due, at least in part, to the effects of de-myelination.

Also of note, Fjell et al., (2008) proposed that FA may be a marker of atrophy that precedes measurable volumetric white matter reductions. Thus, our previous finding of volume reduction in FESZ, which was limited to central CC (del Re et al., 2016a), combined with the current finding of FA abnormalities across all regions of CC in FESZ, would seem to support Fjell et al.'s proposal that diffusion measures may be a more sensitive measure of impending volume loss, as diffusion measures tap into microstructural abnormalities, as opposed to volume measures that tap into macrostructural abnormalities. Microstructural findings may therefore predate macrostructural findings and be important for early intervention. Furthermore, findings from the current study showed decreased FA_t of central CC, which was associated with an increase in positive symptoms. It is noteworthy here that the del Re et al. study (2016a) also reported central CC volume reduction and correlations with positive symptoms but this study did not show other subdivisions of CC as abnormal as was the case in the current study. These findings suggest a role of the central CC in psychosis, or perhaps an earlier detection of abnormalities with more sensitive diffusion measures. Conducting a similar study in later stages of the illness would

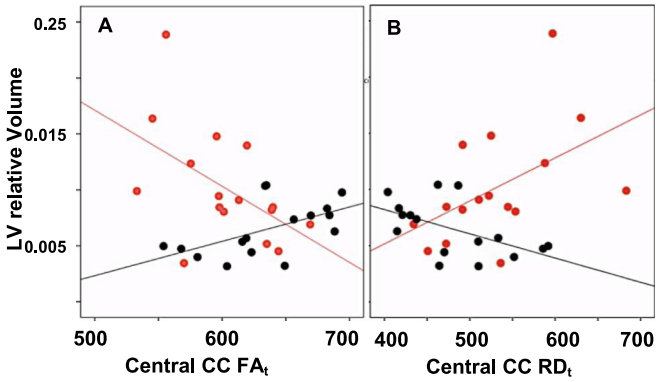

Fig. 4. Correlations between diffusion measures of the central CC and relative volume of bilateral LV in FESZ and HC. **A.** In FESZ (red dots and red least square fit), abnormally decreased FA_t is significantly and negatively correlated with abnormally increased volume of LV. The same correlation in HC is significant but positive (black dots and black least square fit); **B.** In FESZ, abnormally increased RD_t is significantly and positively correlated with increased LV volume (red); In HC, the correlation is negative. Notice that the range of values in FESZ for both diffusion measures is much wider than that observed in HC. (For interpretation of the references to color in this figure legend, the reader is referred to the web version of this article.)

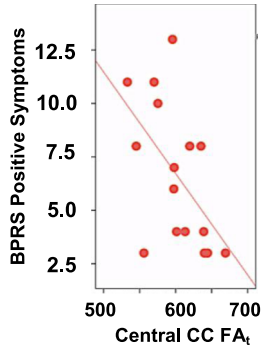

Fig. 5. FA_t of central CC significantly and negatively correlated with positive symptoms score in FESZ ($r = -0.55$, $p < 0.05$), i.e., the more decreased FA_t, the higher the positive symptom score in patients.

likely provide more information regarding whether other subdivisions of the CC besides the central CC, would also show clinical correlates over time.

In addition to identifying abnormalities in the FA_t, RD_t and $trace_t$ of the CC, we also explored the association between these measures and LV volume. Since there is a common genetic link between the volume of CC and the LV (Pfefferbaum et al., 2000; Narr et al., 2000), and CC volume depends on white matter integrity, the relationship between LV and CC might extend to CC diffusion measures. Our findings tend to support this assumption. More specifically, in FESZ, the volume of the LV was negatively correlated with FA_t and positively correlated with RD_t, i.e., increased LV volume was associated with decreased FA_t, and increased RD_t. In healthy controls, the opposite pattern was observed: there was a significant positive correlation between LV volume and FA_t, and a negative correlation with RD_t; i.e., increased LV volume correlated with increased RD, suggesting perhaps more CC myelination and more organization of CC white matter fibers.

Regarding possible links between CC FA white matter reductions in the brain and genes, it is of interest that Vogel et al. (2018) have shown an association between FA white matter reductions and the MIR137 SZ risk variant in individuals at familial high risk for schizophrenia. Of further note, MIR137 regulates genetic pathways involved in both glio- and neurogenesis, further suggesting the involvement of MIR137 in neurodevelopment and in neurodevelopmental syndromes, the latter including both LV and CC structures (Wright et al., 2015). Future studies need to follow up on this potential association. Future studies need to follow up on this potential association.

There are nonetheless limitations to the present study. First, the number of participants is relatively small. A larger sample size is needed to confirm these findings. Second, the majority of FESZ were medicated with psychotropic medications. While we did not find correlations between the variables under study and chlorpromazine equivalents, the effect of medication cannot be completely discounted. Third, the small number of subjects did not make it possible to determine gender effects, and thus further investigation of possible gender effects on diffusion measures of the CC is warranted, given the fact that even early structural measures of CC have shown gender differences (e.g., Hoff et al., 1994).

In summary, and as noted in the Introduction, several inconsistent results for FA abnormalities in CC have been reported in the literature. For example, some studies of FESZ report FA abnormalities of the genu (Lee et al., 2013; Price et al., 2007), while others report abnormalities specific to the splenium of the CC (Dekker et al., 2010). As discussed above, these inconsistent results may be due to the DTI methods used that did not account for the complex CC fiber architecture, or for CSF contamination. It is also of interest that all subdivisions of CC showed diffusion tractography differences between FESZ and controls in this study (microstructural level), although only the central region of the CC was shown to differ in volume in a previous study (macrostructural level) by our group (del Re et al., 2016). Furthermore, robust correlations between several diffusion measures and the LV volume were observed only for the central CC. In addition, correlations between FA_t and clinical symptoms were also observed only for central CC. As described above, these results may suggest that the closest link between LV and CC exists for its central subdivision, and/or that the central CC either plays a particular role in symptom development, or that its microstructural abnormality achieved sufficient severity to impact clinical and functional symptoms. However, since the relationship between changes in central CC and symptoms is correlational, the causality cannot be inferred with confidence and future studies are need to address this question. Moreover, future longitudinal studies are needed to test the possibility that other CC subregions may show similar characteristics over time, as discussed above.

Acknowledgments

We acknowledge the support of Drs. Larry Seidman (LJS; deceased), Robert McCarley (RWM; deceased) as leaders on the Boston CIDAR (see below), and Drs. Jun Konishi, and Yoshio Hirayasu for their early input on previous drafts of this manuscript. This work was funded in part by an NIH Mental Health Centers for Interventional Development and Applied Research grant (Boston CIDAR; NIH/MH 1P50 080272; Project PI RWM and Core PIs: LJS, MES, TP, Drs. Jill Goldstein and Wilson Wu), by an R21 Award from NIMH (R21MH 109819; EDR), and by VA Merit Award support (RWM, MES, MN).

Supplementary materials

Supplementary material associated with this article can be found, in the online version, at doi:10.1016/j.psychres.2019.02.038.

References

Arnone, D., McIntosh, A.M., Tan, G.M., Ebmeier, K.P., 2008. Meta-analysis of magnetic resonance imaging studies of the corpus callosum in schizophrenia. Schizophr. Res. 101 (1–3), 124–132.

Balevich, E.C., Haznedar, M.M., Wang, E., Newmark, R.E., Bloom, R., Schneiderman, J.S., Aronowitz, J., Tang, C.Y., Chu, K.W., Byne, W., Buchsbaum, M.S., Hazlett, E.A., 2015. Corpus callosum size and diffusion tensor anisotropy in adolescents and adults with schizophrenia. Psychiatry Res. 231 (3), 244–251.

Basser, P.J., Jones, D.K., 2002. Diffusion-tensor MRI: theory, experimental design and data analysis—a technical review. NMR Biomed. 15 (7–8), 456–467.

Basser, P.J., Mattiello, J., LeBihan, D., 1994. MR diffusion tensor spectroscopy and imaging. Biophys. J. 66 (1), 259–267.

Basser, P.J., Pierpaoli, C., 1996. Microstructural and physiological features of tissues elucidated by quantitative-diffusion-tensor MRI. J. Magn. Reson. 111 (3), 209–219.

Baumgartner, C., Micahilovich, O., Pasternak, O., Levitt, J., Weston, C.-F., Shenton, M.E., et al., 2012. A unified tractography framework for comparing diffusion models on clinical scans. In: Paper presented at the CDMRI-workshop (MICCAI'12). London, UK.

Buchsbaum, M.S., Friedman, J., Buchsbaum, B.R., Chu, K.W., Hazlett, E.A., Newmark, R., Schneiderman, J.S., Torosjan, Y., Tang, C., Hof, P.R., Stewart, D., Davis, K.L., Gorman, J., 2006. Diffusion tensor imaging in schizophrenia. Biol. Psychiatry 60 (11), 1181–1187.

de Moura, M.T.M., Zanetti, M.V., Duran, F.L.S., Schaufelberger, M.S., Menezes, P.R., Scazufca, M., Busatto, G.F., Serpa, M.H., 2018. Corpus callosum volumes in the 5years following the first-episode of schizophrenia: effects of antipsychotics, chronicity and maturation. NeuroImage Clin. 18, 932–942.

Dekker, N., Schmitz, N., Peters, B.D., van Amelsvoort, T.A., Linszen, D.H., de Haan, L., 2010. Cannabis use and callosal white matter structure and integrity in recent-onset schizophrenia. Psychiatry Res. 181 (1), 51–56.

Del Re, E.C., Konishi, J., Bouix, S., Blokland, G.A., Mesholam-Gately, R.I., Goldstein, J., Kubicki, M., Wojcik, J., Pasternak, O., Seidman, L.J., Petryshen, T., Hirayasu, Y., Niznikiewicz, M., Shenton, M.E., McCarley, R.W., 2016a. Enlarged lateral ventricles inversely correlate with reduced corpus callosum central volume in first episode schizophrenia: association with functional measures. Brain Imaging Behav. 10 (4), 1264–1273.

Del Re, E.C., Gao, Y., Eckbo, R., Petryshen, T.L., Blokland, G.A., Seidman, L.J., Konishi, J., Goldstein, J.M., McCarley, R.W., Shenton, M.E., Bouix, S., 2016b. A new MRI masking technique based on multi-atlas brain segmentation in controls and schizophrenia: a rapid and viable alternative to manual masking. J. Neuroimaging 26 (1), 28–36.

DeLisi, L.E., Sakuma, M., Tew, W., Kushner, M., Hoff, A.L., Grimson, R., 1997. Schizophrenia as a chronic active brain process: a study of progressive brain

structural change subsequent to the onset of schizophrenia. Psychiatry Res. 74 (3), 129–140.
Faul, F., Erdfelder, E., Lang, A.G., Buchner, A., 2007. G*Power 3: a flexible statistical power analysis program for the social, behavioral, and biomedical sciences. Behav. Res. Methods 39 (2), 175–191.
Federspiel, A., Begre, S., Kiefer, C., Schroth, G., Strik, W.K., Dierks, T., 2006. Alterations of white matter connectivity in first episode schizophrenia. Neurobiol. Dis. 22 (3), 702–709.
First, M.B., Pincus, H.A., 2002. The DSM-IV Text Revision: rationale and potential impact on clinical practice. Psychiatric Serv. 53 (3), 288–292.
Fischl, B., Salat, D.H., Busa, E., Albert, M., Dieterich, M., Haselgrove, C., van der Kouwe, A., Killiany, R., Kennedy, D., Klaveness, S., Montillo, A., Makris, N., Rosen, B., Dale, A.M., 2002. Whole brain segmentation: automated labeling of neuroanatomical structures in the human brain. Neuron 33 (3), 341–355.
Fitzsimmons, J., Kubicki, M., Shenton, M.E., 2013. Review of functional and anatomical brain connectivity findings in schizophrenia. Curr. Opin. Psychiatry 26 (2), 172–187.
Fjell, A.M., Westlyea, L.T., Greve, D.N., Fischl, B., Benner, T., van der Kouwec, A.J.W., Salat, D., Bjørnerud, A., Paulina Due-Tønnesseng, P., Walhovd, K.B., 2008. The relationship between diffusion tensor imaging and volumetry as measures of white matter properties. Neuroimage. 42 (4), 1654–1668 October 1.
Francis, A.N., Bhojraj, T.S., Prasad, K.M., Kulkarni, S., Montrose, D.M., Eack, S.M., Keshavan, M.S., 2011. Abnormalities of the corpus callosum in non-psychotic high-risk offspring of schizophrenia patients. Psychiatry Res. 191 (1), 9–15.
Giedd, J.N., Rumsey, J.M., Castellanos, F.X., Rajapakse, J.C., Kaysen, D., Vaituzis, A.C., Vauss, Y.C., Hamburger, S.D., Rapoport, J.L., 1996. A quantitative MRI study of the corpus callosum in children and adolescents. Brain Res. Dev. Brain Res. 91 (2), 274–280.
Hien, D., Matzner, F.J., First, M.B., Spitzer, R.L., Williams, J., Gibbon, M., 1994. Structured clinical interview for DSM-IV childhood diagnoses (KID-SCID). In: Biometrics Research presentation. New York.
Hofer, S., Frahm, J., 2006. Topography of the human corpus callosum re-visited—comprehensive fiber tractography using diffusion tensor magnetic resonance imaging. NeuroImage 32 (3), 989–994.
Hoff, A.L., Neale, C., Kushner, M., DeLisi, L.E., 1994. Gender differences in corpus callosum size in first episode schizophrenic patients. Biol. Psychiatry 35, 913–919.
Hollingshead, A.A., 1975. Four-factor Index of Social Status. Yale University, New Haven, CT.
Hutchinson, A.D., Mathias, J.L., Jacobson, B.L., Ruzic, L., Bond, A.N., Banich, M.T., 2009. Relationship between intelligence and the size and composition of the corpus callosum. Exp. Brain Res. 192 (3), 455–464.
Jones, S.H., Thornicroft, G., Coffey, M., Dunn, G., 1995. A brief mental health outcome scale-reliability and validity of the Global Assessment of Functioning (GAF). Br. J. Psychiatry 166 (5), 654–659.
Keller, A., Jeffries, N.O., Blumenthal, J., Clasen, L.S., Liu, H., Giedd, J.N., Rapoport, J.L., 2003. Corpus callosum development in childhood-onset schizophrenia. Schizophr. Res. 62 (1–2), 105–114.
Kubicki, M., Shenton, M.E., 2015. Editorial to special issue on "white matter pathology". Schizophr. Res. 161 (1), 1–3.
Kubicki, M., Styner, M., Bouix, S., Gerig, G., Markant, D., Smith, K., Kikinis, R., McCarley, R.W., Shenton, M.E., 2008. Reduced interhemispheric connectivity in schizophrenia-tractography based segmentation of the corpus callosum. Schizophr. Res. 106 (2–3), 125–131.
Kubicki, M, McCarley, R, Westin, CF, Park, HJ, Maier, S, Kikinis, R, Jolesz, FA, Shenton, ME, 2007. A review of diffusion tensor imaging studies in schizophrenia. J. Psychiatr. Res. 41 (Jan–Feb (1–2)), 15–30.
Lee, S.H., Kubicki, M., Asami, T., Seidman, L.J., Goldstein, J.M., Mesholam-Gately, R.I., McCarley, R.W., Shenton, M.E., 2013. Extensive white matter abnormalities in patients with first-episode schizophrenia: a Diffusion Tensor Iimaging (DTI) study. Schizophr. Res. 143 (2–3), 231–238.
Luders, E., Narr, K.L., Bilder, R.M., Thompson, P.M., Szeszko, P.R., Hamilton, L., Toga, A.W., 2007. Positive correlations between corpus callosum thickness and intelligence. NeuroImage 37 (4), 1457–1464.
Luders, E., Thompson, P.M., Narr, K.L., Zamanyan, A., Chou, Y.Y., Gutman, B., Dinov, I.D., Toga, A.W., 2011. The link between callosal thickness and intelligence in healthy children and adolescents. NeuroImage 54 (3), 1823–1830.
Malcolm, J.G., Michailovich, O., Bouix, S., Westin, C.F., Shenton, M.E., Rathi, Y., 2010. A filtered approach to neural tractography using the Watson directional function. Med. Image Anal. 14 (1), 58–69.
Metzler-Baddeley, C., O'Sullivan, M.J., Bells, S., Pasternak, O., Jones, D.K., 2012. How and how not to correct for CSF-contamination in diffusion MRI. NeuroImage 59 (2), 1394–1403.
Narr, K.L., Thompson, P.M., Sharma, T., Moussai, J., Cannestra, A.F., Toga, A.W., 2000. Mapping morphology of the corpus callosum in schizophrenia. Cereb. Cortex 10 (1), 40–49.
Overall, J.E., Gorham, D.R., Shawver, J.R., 1961. Basic dimensions of change in the symptomatology of chronic schizophrenics. J. Abnorm. Soc. Psychol. 63, 597–602.
Pasternak, O., Kelly, S., Sydnor, V.J., Shenton, M.E., 2018. Advances in microstructural diffusion neuroimaging for psychiatric disorders. NeuroImage 182, 259–282.
Pasternak, O, Westin, CF, Dahlben, B, et al., 2015. The extent of diffusion MRI markers of neuroinflammation and white matter deterioration in chronic schizophrenia. Schizophr. Res. 161 (1), 113–118.
Pasternak, O., Shenton, M.E., Westin, C.F., 2012a. Estimation of extracellular volume from regularized multi-shell diffusion MRI. Med. Image Comput. Computer-assisted Interv. 15 (Pt 2), 305–312.
Pasternak, O., Westin, C.F., Bouix, S., Seidman, L.J., Goldstein, J.M., Woo, T.U., Petryshen, T.L., Mesholam-Gately, R.I., McCarley, R.W., Kikinis, R., Shenton, M.E., Kubicki, M., 2012b. Excessive extracellular volume reveals a neurodegenerative pattern in schizophrenia onset. J. Neurosci. 32 (48), 17365–17372.
Pasternak, O, Sochen, B, Gur, Y, et al., 2009. Free water elimination and mapping from diffusion MRI. Magn. Res. Med. 62 (3), 717–730.
Paul, L.K., 2011. Developmental malformation of the corpus callosum: a review of typical callosal development and examples of developmental disorders with callosal involvement. J. Neurodev. Disord. 3 (1), 3–27.
Pfefferbaum, A., Sullivan, E.V., Swan, G.E., Carmelli, D., 2000. Brain structure in men remains highly heritable in the seventh and eighth decades of life. Neurobiol, Aging 21 (1), 63–74.
Pieper, S., Halle, M., Kikinis, R., 2004. 3D slicer. In: 2004 2nd IEEE International Symposium on Biomedical Imaging: Nano to Macro (IEEE Cat No. 04EX821). Arlington, VA, USA. 1. pp. 632–635 2004.
Pieper, S., Lorensen, B., Schroeder, W., Kikinis, R., 2006. The NA-MIC Kit: ITK, VTK, pipelines, grids and 3D slicer as an open platform for the medical image computing community. In: 3rd IEEE International Symposium on Biomedical Imaging: Nano to Macro, 2006. Arlington, VA. pp. 698–701.
Prendergast, D.M., Ardekani, B., Ikuta, T., John, M., Peters, B., DeRosse, P., Wellington, R., Malhotra, A.K., Szeszko, P.R., 2015. Age and sex effects on corpus callosum morphology across the lifespan. Human Brain Mapp. 36 (7), 2691–2702.
Price, G., Bagary, M.S., Cercignani, M., Altmann, D.R., Ron, M.A., 2005. The corpus callosum in first episode schizophrenia: a diffusion tensor imaging study. J. Neurol., Neurosurg. Psychiatry 76 (4), 585–587.
Price, G., Cercignani, M., Parker, G.J., Altmann, D.R., Barnes, T.R., Barker, G.J., Joyce, E.M., Ron, M.A., 2007. Abnormal brain connectivity in first-episode psychosis: a diffusion MRI tractography study of the corpus callosum. NeuroImage 35 (2), 458–466.
Pujol, J., Vendrell, P., Junque, C., Marti-Vilalta, J.L., Capdevila, A., 1993. When does human brain development end? Evidence of corpus callosum growth up to adulthood. Annals Neurol. 34 (1), 71–75.
Rotarska-Jagiela, A., Schonmeyer, R., Oertel, V., Haenschel, C., Vogeley, K., Linden, D.E., 2008. The corpus callosum in schizophrenia-volume and connectivity changes affect specific regions. NeuroImage 39 (4), 1522–1532.
Song, S.K., Sun, S.W., Ju, W.K., Lin, S.J., Cross, A.H., Neufeld, A.H., 2003. Diffusion tensor imaging detects and differentiates axon and myelin degeneration in mouse optic nerve after retinal ischemia. NeuroImage 20 (3), 1714–1722.
Song, S.K., Sun, S.W., Ramsbottom, M.J., Chang, C., Russell, J., Cross, A.H., 2002. Dysmyelination revealed through MRI as increased radial (but unchanged axial) diffusion of water. NeuroImage 17 (3), 1429–1436.
Song, S.K., Yoshino, J., Le, T.Q., Lin, S.J., Sun, S.W., Cross, A.H., Armstrong, R.C., 2005. Demyelination increases radial diffusivity in corpus callosum of mouse brain. NeuroImage 26 (1), 132–140.
Vogel, B.O., Lett, T.A., Erk, S., Mohnke, S., Wackerhagen, C., Brandl, E.J., Romanszuk-Seiferth, N., Otto, K., Schweiger, J.I., Tost, H., Nothen, M.M., Rietschel, M., Degenhardt, F., Witt, S.H., Meyer-Lindenberg, A., Heinz, A., Walter, H., 2018). The influence of MIR137 on white matter fractional anisotropy and cortical surface area in individuals with familial risk for psychosis. Schizophr Res 195, 190–196.
Wechsler, D., 1999. Wechsler Abbreviated Scale of Intelligence. Psychological Corporation, Harcourt Brace.
Whitford, T.J., Ford, J.M., Mathalon, D.H., Kubicki, M., Shenton, M.E., 2012. Schizophrenia, myelination, and delayed corollary discharges: a hypothesis. Schizophr. Bull. 38 (3), 486–494.
Wilkinson, G.S., Robertson, G.J., 2006. Wide Range Achievement Test 4 Professional Manual. Psychological Assessment Resources, Lutz, FL.
Woodruff, P.W., McManus, I.C., David, A.S., 1995. Meta-analysis of corpus callosum size in schizophrenia. J. Neurol., Neurosurg. Psychiatry 58 (4), 457–461.
Wright, C., Calhoun, V.D., Ehrlich, S., Wang, L., Turner, J.A., Bizzozero, N.I., 2015. Meta gene set enrichment analyses link miR-137-regulated pathways with schizophrenia risk. Front. Genet. 6, 147.
Zhuo, C., Liu, M., Wang, L., Tian, H., Tang, J., 2016. Diffusion tensor MR Imaging evaluation of callosal abnormalities in schizophrenia: a meta-analysis. PloS One 11 (8), e0161406.